

Application of SAGE algorithm in PET image reconstruction using modified ordered subsets

Zhu Hongqing Shu Huazhong Zhou Jian Luo Limin

(Department of Biological Science and Medical Engineering, Southeast University, Nanjing 210096, China)

Abstract: A new method that uses a modified ordered subsets (MOS) algorithm to improve the convergence rate of space-alternating generalized expectation-maximization (SAGE) algorithm for positron emission tomography (PET) image reconstruction is proposed. In the MOS-SAGE algorithm, the number of projections and the access order of the subsets are modified in order to improve the quality of the reconstructed images and accelerate the convergence speed. The number of projections in a subset increases as follows: 2, 4, 8, 16, 32 and 64. This sequence means that the high frequency component is recovered first and the low frequency component is recovered in the succeeding iteration steps. In addition, the neighboring subsets are separated as much as possible so that the correlation of projections can be decreased and the convergences can be speeded up. The application of the proposed method to simulated and real images shows that the MOS-SAGE algorithm has better performance than the SAGE algorithm and the OSEM algorithm in convergence and image quality.

Key words: positron emission tomography; space-alternating generalized expectation-maximization; image reconstruction; modified ordered subsets

Iterative image reconstruction is known to be a slow process, which means that many iteration steps are required to obtain precise images. With the maximum likelihood-expectation maximization (ML-EM) algorithm, a precise PET reconstructed image requires more than 80 steps^[1]. An ordered subsets (OS) algorithm is a useful method to accelerate image reconstruction for the ML-EM method^[2]. The ML-EM method combined with the OS algorithm is called the OSEM method.

The EM algorithm converges globally, but slowly^[3]. This is because the convergence rate of the EM algorithm is inversely related to the Fisher information of its complete data space^[4]. In Refs. [5, 6], the authors proposed the space-alternating generalized EM (SAGE) algorithm in which the parameters are updated sequentially using a sequence of small “hidden” data spaces rather than one large complete-data space. By choosing “hidden” data spaces with considerably less Fisher information, the SAGE algorithm converges faster than the EM algorithm^[4,5]. Less informative “hidden” data spaces can yield fast convergence. SAGE acceleration is based fundamentally on statistical considerations, so monotonic increases in the objective function and global convergence are guaranteed^[4].

In this paper, a new algorithm, namely MOS-

SAGE that combines a modified OS algorithm with the SAGE algorithm is proposed for PET image reconstruction. As we all know, the quality of the reconstructed images using an OS method depends upon several factors such as the projection data that consist of subsets, the access order of the subsets, and the number of subsets. In order to improve it, we modify the number of projections and the access order in each subset iteration step. The purpose is to recover the higher and lower frequency components in iteration steps and to decrease the influence of noise. To demonstrate the effectiveness of the proposed method, we apply it to some simulated and real images. Experimental results show that it is superior to the SAGE and OSEM algorithms, even for those images with Poisson noise.

1 Methodology

1.1 MOS-SAGE algorithm

The OS principle can be used in any algorithm that involves sums over sinogram indices. Since the SAGE algorithm contains sums over sinogram indices, we try to apply the OS idea to this algorithm, and then we adjust the number of projections and the access order of the subsets.

Let $S', t = 1, 2, \dots, n$, be the ordered subsets, where n is the subset number. The MOS-SAGE algorithm can be outlined as follows:

Initialization: Let \hat{x}^1 be a positive starting image vector.

For each iteration $m = 1, 2, \dots$ until convergence

Received 2005-03-21.

Foundation item: The National Basic Research Program of China (973 Program) (No. 2003CB716102).

Biographies: Zhu Hongqing (1967—), female, doctor, hqzhu@sjtu.edu.cn; Shu Huazhong (corresponding author), male, professor, shu.list@seu.edu.cn.

of $\hat{\mathbf{x}}^m$, where $\hat{\mathbf{x}}^m$ denotes the estimate of \mathbf{x} after m iterations.

For each subset $t = 1, 2, \dots, n$ (loop on subsets)

For a given subset, setup a starting image vector:
 $\mathbf{x}^m = \hat{\mathbf{x}}^t$.

For the given subset and starting image vector, calculate the initialize projection:

$$\bar{y}_j^t = \sum_i a_{ji} x_i^m + r_j^t \quad j \in S^t; i = 1, 2, \dots, I \quad (1)$$

where I is the dimension of the image space. Elements of system matrix a_{ji} represent the probability that an emission from pixel i is recorded at detector j , and x_i^m is the expected value of pixel i at the m -th iteration. For simplicity, r_j^t is assumed to be zero^[4].

For image space, $k = 1, 2, \dots, I$ (loop on image space)

Calculate error partition:

$$e_k^t = \sum_j a_{jk} \frac{y_j^t}{\bar{y}_j^t} \quad j \in S^t \quad (2)$$

Update the pixel value:

$$x_k^{m+1} = x_k^m \frac{e_k^t}{\sum_j a_{jk}} \quad j \in S^t \quad (3)$$

$$x_l^{m+1} = x_l^m \quad l \neq k \quad (4)$$

Update projection on subsets:

$$\bar{y}_j^t = \bar{y}_j^t + (x_k^{m+1} - x_k^m) a_{jk} \quad \forall j, a_{jk} \neq 0 \quad (5)$$

Endfor

For the next subset, we take

$$\hat{\mathbf{x}}^{t+1} = \mathbf{x}^{m+1} \quad (6)$$

Endfor

Endfor

From the new MOS-SAGE algorithm described above, we can see that the OS version SAGE updates projection data sequentially. But the OS version ML-EM algorithm waits until all project data have been updated. Although the OS technique can also be applied in ML-EM (OSEM) and in SAGE (MOS-SAGE), the inner merit of SAGE is better than EM. So in view of the convergence speed, MOS-SAGE is faster than OS-EM and SAGE.

1.2 Access order of the subsets

According to Refs. [2, 7, 8], the projection access order has also an influence on the convergence rate of the iteration. The greater the correlation of projections is, the slower the convergence rate of the iteration is. In Ref. [3], it was shown that it is advantageous to select subsets in a balanced way so that pixels actively contribute equally to any subsets. Therefore, we adjust the projection access order in order to separate the neighboring subsets as much as possible so that we can decrease the correlation of projections. We select the access order of the subsets shown in Fig. 1. For simplicity,

eight projections in a subset level are considered in this example.

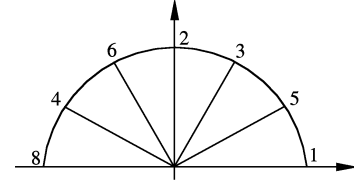


Fig. 1 Access orders for eight projections in this example

1.3 Selection of projection data

In the OS method, projection data in a subset are playing a key role in image reconstruction, especially for the images with noise. In Ref. [9], the authors described a wonderful method of selecting projection data for each iteration step. We propose here an improvement on their method. If the number of projections is 64, the number of projections in a subset increases as follows: 2, 4, 8, 16, 32, and 64. This sequence means the high frequency component is recovered first and the low frequency component is recovered in the succeeding iteration steps. For small subset level (many projections in each subset), the constructed images are insensitive to noise. The reason is that a pixel value is modified by a lot of projections and the effect of noise is averaged in an iteration process^[9, 10]. In our MOS-SAGE algorithm, we adopt such a strategy.

2 Evaluation Criteria

Several quantitative evaluation methods are used to test some reconstructed algorithms.

1) Correlation coefficient

The correlation coefficient ε_1 is defined as

$$\varepsilon_1 = \frac{\sum_{i=1}^I (x_i^{\text{rec}} - \bar{x}^{\text{rec}})(x_i^{\text{tes}} - \bar{x}^{\text{tes}})}{\left[\sum_{i=1}^I (x_i^{\text{rec}} - \bar{x}^{\text{rec}})^2 \sum_{i=1}^I (x_i^{\text{tes}} - \bar{x}^{\text{tes}})^2 \right]^{\frac{1}{2}}} \quad (7)$$

where \bar{x}^{rec} and \bar{x}^{tes} are the average gray levels of reconstructed image and test reference image, respectively; ε_1 indicates the spatial similarity between the test reference images and reconstructed images. The best algorithm will have the maximum value of ε_1 .

2) Normalized mean square error

The normalized mean square error is defined as

$$\varepsilon_2 = \left[\frac{\sum_{i=1}^I (x_i^{\text{tes}} - x_i^{\text{rec}})^2}{\sum_{i=1}^I (x_i^{\text{tes}} - \bar{x}^{\text{tes}})^2} \right]^{\frac{1}{2}} \quad (8)$$

where x_i^{tes} is the test image gray level for pixel element i , x_i^{rec} is the reconstructed image gray level for the pixel element i , and \bar{x}^{tes} is the average gray level of the test image. The best algorithm will have the minimum val-

ue of the normalized mean square error. ε_2 is sensitive to big errors of a few elements.

3) Normalized mean absolute error

The normalized mean absolute error is defined as

$$\varepsilon_3 = \frac{\sum_{i=1}^I |x_i^{\text{tes}} - x_i^{\text{rec}}|}{\sum_{i=1}^I |x_i^{\text{tes}}|} \quad (9)$$

The best algorithm will have the minimum value of ε_3 . It is sensitive to small errors of many elements.

4) Mean absolute error

The mean absolute error (MAE) is defined as

$$\varepsilon_4 = \frac{1}{I} \sum_{i=1}^I |x_i^{\text{tes}} - x_i^{\text{rec}}| \quad (10)$$

ε_4 measures the average discrepancy between a reconstructed image and the test image.

3 Experimental Results

To assess the effectiveness and speed of the new MOS-SAGE algorithm, we present reconstructed results using OSEM, SAGE and MOS-SAGE. The Shepp-Logan digital phantom shown in Fig. 2 was the object we tested. Reconstruction is based on projection data obtained from Matlab 6.5. Therefore, its projections are known theoretically. For the sake of simplicity, the attenuation coefficients were not taken into account in this experiment. The reconstructed images were 64×64 pixel matrices. The sinogram had 95 radial bins and 180 angles. The total photon counts amounted to 95×180 . Fig. 2(b) shows the Shepp-Logan phantom with uniform Poisson noise in projection data (5%).



Fig. 2 Test image. (a) Shepp-Logan phantom; (b) Shepp-Logan phantom with Poisson ratio (5%)

The reconstructed images are shown in Fig. 3. From top to bottom, the odd rows are noise free, and the even rows have Poisson noise (5%). Figs. 3(a) and (c) are the SAGE algorithm, the iteration numbers are 10; Figs. 3(b) and (d) are the SAGE algorithm, the iteration numbers are 30; Figs. 3(e) to (h) are the OSEM algorithm; Figs. 3(i) to (l) are the MOS-SAGE algorithm; Figs. 3(e), (g), (i) and (k) have iteration numbers 2. Figs. 3(f), (h), (j) and (l) have iteration numbers 6.

Figs. 3(a) to (d) show the reconstructed images using the SAGE method. The iteration numbers of the

first column and the second column are 10 and 30, respectively. In all the OS steps, the access order of the subsets uses the method described in section 1.2. The iteration numbers of the first column in OS methods are 2 and the last column are 6. The sequence of the number of projections in each subset is 2, 4, 8, 16, 32, and 64, respectively.

Fig. 3 shows clearly that the MOS-SAGE converges faster than the SAGE; this is due to the fact that the OS technique permits us to accelerate the convergence.

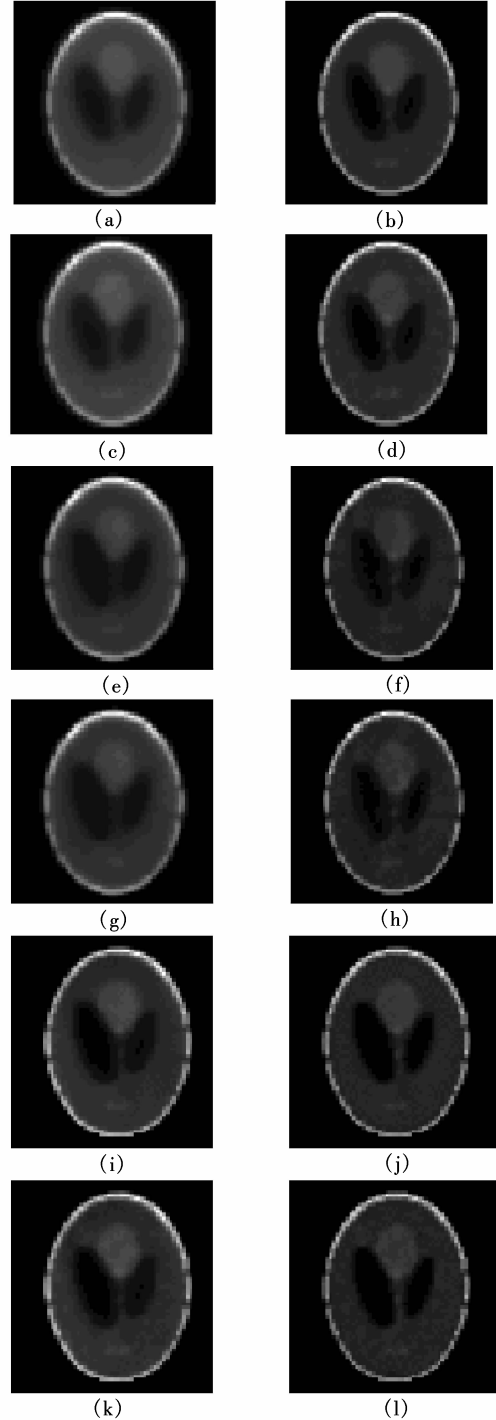


Fig. 3 Reconstructions using simulated Shepp-Logan phantom

We can also observe that the MOS-SAGE is more efficient than the OSEM. This can be explained by the fact that in the former algorithm, only a sequence of small “hidden” data spaces rather than one large complete data space were taken into account, but in the latter algorithm, the Fisher information of the complete data space was used.

In considering the noise free and the Poisson noise projections, we find the reconstructed images where the same conditions are similar. The reason is probably that all reconstructed methods are based on statistic consideration on one hand; and on the other hand the modified OS technique also improves the quality of images.

The proposed MOS-SAGE yields some high quality reconstructed images in comparison with two other methods (OSEM and SAGE). This can be confirmed by the results shown in Fig. 4 from which we can observe that the reconstructed result obtained at 6 iterations using the MOS-SAGE is similar to those obtained using the OSEM or the SAGE at 30 iterations.

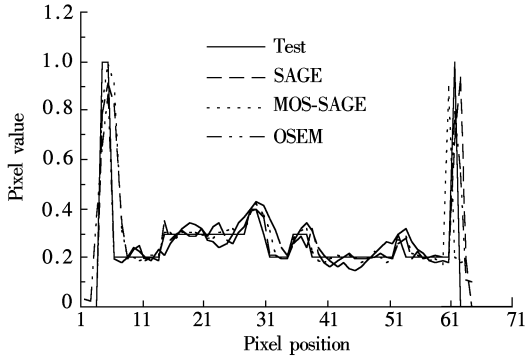


Fig. 4 Profiles of images reconstructed by several algorithms

For objective and quantitative evaluation of the reconstructed images, we use the criteria described in section 2. Tab. 1 shows the reconstruction errors using different criteria for different algorithms. We can observe from Tab. 1 that the reconstructed images obtained by the MOS-SAGE are superior to those by the two other methods.

Tab. 1 Quantitative comparison of several algorithms versus iteration numbers

Algorithm	ε_1	ε_2	ε_3	ε_4	Iteration number
SAGE	0.732 0	0.986 4	1.139 7	0.118 9	10
SAGE	0.789 4	0.890 0	0.894 9	0.114 2	30
OSEM	0.591 8	0.971 8	1.443 7	0.221 2	2
OSEM	0.593 4	0.890 9	1.134 2	0.219 6	6
MOS-SAGE	0.836 5	0.893 0	1.126 4	0.118 7	2
MOS-SAGE	0.883 1	0.871 4	0.971 5	0.108 8	6

The MOS-SAGE was also applied to real PET transmission scan projection data. The projection space was 160 radial bins and 192 angles, and the reconstructed

images were 128×128 . The reconstructed images using the SAGE, OSEM and MOS-SAGE are shown in Fig. 5. OS parameters’ selection is the same as that used in the above experiment.

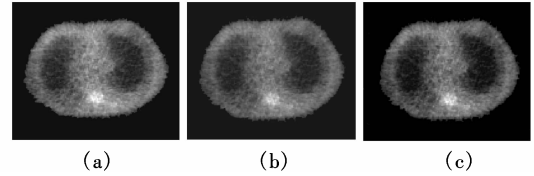


Fig. 5 Reconstructions using clinical PET transmission scan data. (a) SAGE (iteration numbers 30); (b) OSEM (iteration numbers 6); (c) MOS-SAGE (iteration numbers 6)

Real PET projection data’s reconstructed results are similar to those of computer simulated data (Shepp-Logan digital phantom).

4 Conclusion

We have proposed a new reconstruction algorithm MOS-SAGE that consists of modifying the number of projections in each iteration. Using such a strategy, both the high and low frequency components can be recovered in reconstructed images. Besides low time cost, the simulation results show that the new method is robust to noise and yields good results compared with those of conventional reconstruction methods such as the OSEM and the SAGE. The quantitative evaluation results show clearly that the MOS-SAGE can be effectively used in the image reconstruction process.

References

- [1] Schmidlin P, Bellemann M E, Brix G. Iterative reconstruction of PET images using high-overrelaxation single-projection algorithm [J]. *Phys Med Biol*, 1997, **42**: 569 – 582.
- [2] Hudson H M, Larkin R S. Accelerated image reconstruction using ordered subsets of projection data [J]. *IEEE Trans Med Imag*, 1994, **13**(4): 601 – 609.
- [3] Lange K, Carson R. EM reconstruction algorithm for emission and transmission tomography [J]. *J Comp Assisted Tomography*, 1994, **8**(2): 306 – 316.
- [4] Fessler J A, Hero A O. Space-alternating generalized expectation-maximization algorithm [J]. *IEEE Trans on Signal Processing*, 1994, **42**(10): 2664 – 2676.
- [5] Fessler J A, Hero A O. New complete-data spaces and faster algorithms for penalized-likelihood emission tomography [A]. In: *IEEE Conference on Nuclear Science Symposium and Medical Imaging Conference* [C]. Virginia, 1994. 1897 – 1901.
- [6] Fessler J A, Hero A O. Complete-data spaces and generalized EM algorithms [A]. In: *IEEE International Conference on Acoustics, Speech, and Signal Processing* [C]. Minneapolis, USA, 1993. 1 – 4.
- [7] Takahash M, Ogawa K. Selection of projection set and the

- order of calculation in ordered subsets expectation maximization method [A]. In: *IEEE Conference on Nuclear Science Symposium and Medical Imaging* [C]. Toronto, Canada, 1998. 1408 – 1412.
- [8] Guan H, Gordon R A. Projection access order for speedy convergence of ART (algebraic reconstruction technique): a multilevel scheme for computed tomography [J]. *Phys Med Biol*, 1993, **39**: 2005 – 2020.
- [9] Ogawa K, Urabe H. Image quality in the modified ordered subset-Bayesian reconstruction [A]. In: *IEEE International Conference of Nuclear Science Symposium* [C]. Lyon, France, 2000. 874 – 878.
- [10] Urabe H, Ogawa K. Introduction of ordered subsets algorithm to maximum a posteriori expectation maximization method [A]. In: *IEEE International Conference on Image Processing* [C]. Chicago, USA, 1998, **3**: 394 – 398.

基于改进的有序子集的 SAGE 算法在 PET 图像重建中的应用

朱宏擎 舒华忠 周 健 罗立民

(东南大学生物科学与医学工程系, 南京 210096)

摘要:提出了一种利用修改的有序子集(MOS)方法改进空间交替广义期望最大(SAGE)算法收敛性的方法.新的可变有序子集算法(MOS-SAGE)通过修改投影数据的数目和子集的排列循序加速收敛速度.其中每一个子集中的投影数目按2,4,8,16,32,64来排列以便重建算法首先恢复高频部分信息,然后重建低频部分信息.另外新算法还使相邻子集尽可能分离以减少投影间的相关性,达到加速收敛的效果.实验中,运用MOS-SAGE算法对计算机仿真的PET投影数据和实际的临床数据进行重建.几种误差分析结果表明,MOS-SAGE算法的收敛性能比SAGE算法和有序子集期望最大算法(OS-EM)要快,重建后的图像更接近仿真用的模板图像.

关键词:正电子发射断层成像技术;空间交替广义期望最大;图像重建;改进的有序子集

中图分类号:R817